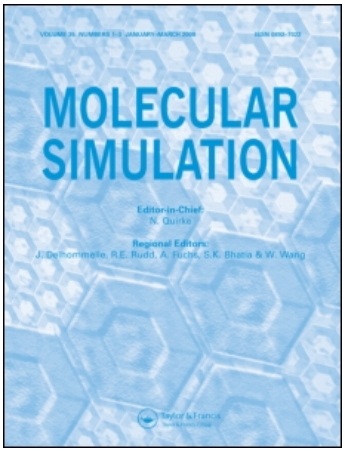

Molecular Simulation
Publication details, including instructions for authors and subscription information:
http://www.informaworld.com/smpp/title~content=t713644482

Shear Viscosity of Model Mixtures by Nonequilibrium Molecular Dynamics. IV. Effect of Molecular Shape

Song Hi Iee[a]; Peter T. Cummings[bc]
[a] Department of Chemistry, Kyungsung University, Pusan, Korea [b] Departments of Chemical Engineering, Chemistry and Computer Science, University of Tennessee, Knoxville, TN, USA [c] Chemical Technology Division, Oak Ridge National Laboratory, Oak Ridge, TN, USA

To cite this Article Iee, Song Hi and Cummings, Peter T.(2001) 'Shear Viscosity of Model Mixtures by Nonequilibrium Molecular Dynamics. IV. Effect of Molecular Shape', Molecular Simulation, 27: 3, 139 — 155
To link to this Article: DOI: 10.1080/08927020108023020
URL: http://dx.doi.org/10.1080/08927020108023020

Molecular Simulation, 2001, Vol. 27, pp. 139–155
Reprints available directly from the publisher
Photocopying permitted by license only

SHEAR VISCOSITY OF MODEL MIXTURES BY NONEQUILIBRIUM MOLECULAR DYNAMICS. IV. EFFECT OF MOLECULAR SHAPE

SONG HI LEE[a,*] and PETER T. CUMMINGS[b,c]

[a]*Department of Chemistry, Kyungsung University, Pusan 608-736, Korea;*
[b]*Departments of Chemical Engineering, Chemistry and Computer Science, University of Tennessee, Knoxville, TN 37996-2200, USA;* [c]*Chemical Technology Division, Oak Ridge National Laboratory, Oak Ridge, TN 37831-6268, USA*

(Received September 2000; accepted September 2000)

We present new results for thermodynamic properties and viscosities of pure dumbbell fluids, spherical/dumbbell mixtures, and dumbbell/dumbbell mixtures. It is evident that the interaction between dumbbell molecules is less attractive than that between spherical molecules which leads to lower viscosities. The shear viscosities and the LJ energies of both spherical Ar/dumbbell Kr (case B) and dumbbell Ar/dumbbell Kr (case C) are described quite well by the liquid mixture expression. The ideality in case C is much better than in case B which is consistent with the idea that dumbbell/dumbbell mixtures are likely to be more ideal than spherical/dumbbell mixtures. But the mixture pressures of the spherical/dumbbell mixture (case B) are described accurately by the ideal liquid mixture expression while those of the dumbbell/dumbbell mixture (case C) are not, which is not consistent with the better ideality of case C in the shear viscosity and the LJ energy than case B.

Keywords: Shear viscosity; Molecular shape; Non-equilibrium

I. INTRODUCTION

In previous papers [1–4], we reported non-equilibrium molecular dynamics (NEMD) calculations of shear viscosities of pure argon and krypton liquids using Lennard-Jones(LJ) and Barker-Fisher Watts(BFW) potentials [5, 6] without considering a three-body potential, and argon/krypton mixtures

*Corresponding author.

using LJ potential [1], pure argon liquid using the highly accurate BFW model both with and without the Axilrod-Teller [7] three-body potential [2], and pure dipolar fluids, nonpolar/polar fluid mixtures, and polar/polar fluid mixtures using LJ plus Stockmayer [8] potentials [3], and pure quadrupolar fluids, a pure dipolar quadrupolar fluid, nonquadrupolar/quadrupolar mixtures, and quadrupolar/quadrupolar mixtures [4]. The goal of theses studies was to clearly delineate the effect of dipolar and quadrupolar interactions on the shear viscosity. Continuing those studies here, we present new results for thermodynamic properties and viscosities of several shapes of dumbbell. By comparing the computed shear viscosity with those from earlier studies, the effect of nonlinear shape on the shear viscosity can be evaluated.

In Section II, we present the brief intermolecular potentials and NEMD algorithm used to calculate the shear viscosity. The results of our simulations are discussed in Section III.

II. SIMULATION DETAILS

The dumbbell molecule is modeled as an atom–atom or site–site model of a diatomic molecule. The total interaction is a sum of pairwise contributions from distinct atoms a in molecule i, at position $\mathbf{r}_{ia}$, and b in molecule j, at position $\mathbf{r}_{jb}$:

$$u_{ij}(r_{ij}) = \sum_{a=1}^{2} \sum_{b=1}^{2} u_{ab}(r_{ab}), \tag{1}$$

where r_{ab} is the inter-site separation $r_{ab} = |\mathbf{r}_{ia} - \mathbf{r}_{jb}|$ and u_{ab} is the pair potential acting between sites a and b:

$$u_{ab}(r_{ab}) = 4\varepsilon_d \left[\left(\frac{\sigma_d}{r_{ab}} \right)^{12} - \left(\frac{\sigma_d}{r_{ab}} \right)^{6} \right]. \tag{2}$$

Here σ_d and ε_d are the Lennard-Jones (LJ) parameters for the dumbbell molecule. The interatomic separation in a dumbbell, l, is chosen such as the volume of the dumbbell molecule is the same as that of a sphere of diameter σ_s. Since the volume of a dumbbell of two spheres of diameter σ_d is given by

$$V_d = \frac{1}{6}\pi\sigma_d^3 + \frac{1}{4}\pi\sigma_d^2 l - \frac{1}{12}\pi l^3, \tag{3}$$

for a given interatomic separation $l = L\sigma_d$, σ_d is determined by equating $V_d = V_s$, and can be expressed in the form of $\sigma_d = c\sigma_s$. In this study, we have chosen as $L = 0$, 1/5, 1/3, and 1/2, and c is determined as 1.0, 0.9172, 0.8772, and 0.8399, respectively. The other LJ parameter ε_d is chosen as $\varepsilon_s/4$. The LJ parameters, σ_s and ε_s, for spherical Ar and spherical Kr are given in Table I. All simulations were carried on 108 molecules fully equilibrated for at least 300,000 time steps of 10^{-15} second(1 fs). The intermolecular potentials were subject to spherical cutoffs as follows: the cutoff distance was 2.25 σ_{Ar} for pure dumbbell Ar, and 2.25 σ_{Kr} for pure fluids and mixtures containing dumbbell Kr.

All simulations reported in this paper was performed in a canonical ensemble. The isochoric isokinetic (NVT) sllod algorithm is obtained simply by putting $\kappa' = 0$ in the isobaric isokinetic (NpT) sllod algorithm [3]. The equations of motion for this algorithm are given by

$$\frac{d\mathbf{r}_i}{dt} = \frac{\mathbf{p}i}{m_i} + \mathbf{r}_i P\,\mathbf{u} \tag{4a}$$

$$\frac{d\mathbf{p}i}{dt} = \mathbf{F}_i - \mathbf{p}i \cdot \nabla\mathbf{u} - \alpha\mathbf{p}i \tag{4b}$$

$$\mathbf{T}_i p = \mathbf{A}_i \mathbf{T}_i \tag{5a}$$

$$\frac{d\mathbf{L}_i p}{dt} = \mathbf{T}_i p \tag{5b}$$

$$\omega_i p = L_i p / I_i, \tag{5c}$$

$$\frac{d}{dt}\begin{pmatrix} q_{i1} \\ q_{i2} \\ q_{i3} \\ q_{i4} \end{pmatrix} = \frac{1}{2}\begin{pmatrix} -q_{i3} & -q_{i4} & q_{i2} & q_{i1} \\ q_{i4} & -q_{i3} & -q_{i1} & q_{i2} \\ q_{i1} & q_{i2} & q_{i4} & q_{i3} \\ -q_{i2} & q_{i1} & -q_{i3} & q_{i4} \end{pmatrix}\begin{pmatrix} w_{ixp} \\ w_{iyp} \\ 0 \\ 0 \end{pmatrix} \tag{5d}$$

TABLE I LJ parameters for Ar/Ar, Kr/Kr, and Ar/Kr interactions

Interaction	σ_s(Å)	ε_s/k_B(°K)
Ar/Ar	3.405	119.8
Kr/Kr	3.633	167.0
Ar/Kr	3.519	141.4

$$
\begin{aligned}
A_{i11} &= -q_{i1}\,q_{i1} + q_{i2}\,q_{i2} - q_{i3}\,q_{i3} + q_{i4}\,q_{i4} \\
A_{i12} &= 2(q_{i3}\,q_{i4} - q_{i1}\,q_{i2}) \\
A_{i13} &= 2(q_{i2}\,q_{i3} + q_{i1}\,q_{i4}) \\
A_{i21} &= -2(q_{i1}\,q_{i2} + q_{i3}\,q_{i4}) \\
A_{i22} &= q_{i1}\,q_{i1} - q_{i2}\,q_{i2} - q_{i3}\,q_{i3} + q_{i4}\,q_{i4} \\
A_{i23} &= 2(q_{i2}\,q_{i4} - q_{i1}\,q_{i3}) \\
A_{i31} &= 2(q_{i2}\,q_{i3} - q_{i1}\,q_{i4}) \\
A_{i32} &= -2(q_{i1}\,q_{i3} + q_{i2}\,q_{i4}) \\
A_{i33} &= -q_{i1}\,q_{i1} - q_{i2}\,q_{i2} + q_{i3}\,q_{i3} + q_{i4}\,q_{i4}
\end{aligned}
\tag{5e}
$$

In Eqs. (4a) and (4b), $\mathbf{r}_i$, m_i, and $\mathbf{p}_i$ are the position, mass, and momentum respectively of molecule i, $\mathbf{F}_i$ is the force exerted by the other molecules on molecule i, $\mathbf{u}=(u_x,0,0)$ with $u_x=\gamma y$ is the velocity field corresponding to planar Couette flow. In Eqs. (5a)–(5e), $\mathbf{L}_i$ is the angular momentum of molecule i and $\mathbf{T}_i$ is the torque on molecule i in the laboratory frame, the superscript p denotes a quantity in the principal axis frame of a molecule, $\mathbf{A}_i$ is the rotation matrix which transforms vectors from the laboratory frame to the principal axis frame of molecule i, the elements of $\mathbf{A}_i$ are given by Eq. (5e), I_{it} is the moment of inertia of molecule i and $q_{i\alpha}$ ($\alpha=1,2,3,4$) are the quaternion parameters related to the Euler angles describing the orientation of molecule i in the laboratory frame

$$e_{ix} = 2(q_{i2}\,q_{i3} - q_{i1}\,q_{i4}) \tag{6a}$$

$$e_{iy} = -2(q_{i1}\,q_{i3} + q_{i2}\,q_{i4}) \tag{6b}$$

$$e_{iz} = -q_{i1}\,q_{i1} - q_{i2}\,q_{i2} + q_{i3}\,q_{i3} + q_{i4}\,q_{i4} \tag{6c}$$

where $e_{i\alpha}$ ($\alpha=x,y,z$) are the components of is the orientational unit vector of molecule i. Note that the quaternions satisfy the normalization $q_{i1}^2 + q_{i2}^2 + q_{i3}^2 + q_{i4}^2 = 1$. The use of quaternions lead to singularity free equations of motion [9, 10]. The parameter α is the thermostating constant, given by

$$\alpha = \frac{\sum_{i=1}^{N}[(\mathbf{p}_i \cdot \mathbf{F}_i - \gamma p_{ix}\,p_{iy})/m_i]}{\sum_{i=1}^{N}[(\mathbf{p}_i \cdot \mathbf{p}_i)/m_i]} \tag{7}$$

The effect of the thermostating term involving $\alpha\mathbf{p}_i$, in Eq. (4b) is to hold the translational kinetic energy constant. The functional form of this term is derived by Gauss's principle of least constraint. The momenta in Eqs. (5a)

and (5b) are measured with respect to the streaming velocity of the fluid and are known as peculiar momenta. The pressure is the trace of the pressure tensor **P**, which is expressed in terms of molecular quantity by

$$\mathbf{P}V = \sum_{i=1}^{N} \mathbf{p}_i \, \mathbf{p}_i / m_i + \sum_{1 < i < j < N} \mathbf{r}_{ij} \, \mathbf{F}_{ij} \tag{8}$$

where V is the volume of the system and is the force between molecules i and j.

These equations of motion are combined with the Lees-Edwards "sliding brick" boundary conditions [11]. In the absence of the thermostat and the isobaric constraint, the terms in Eqs. (4a) and (4b) involving the strain field, $\nabla \mathbf{u}$, cancel to yield Newton's equations of motion relating $\mathbf{r}_i$ and $\mathbf{F}_i$. This implies that the sllod algorithm truly generates boundary driven planar Couette flow, leading to the conclusion that it is correct to arbitrary order in the strain rate [12]. In order to obtain a good signal-to-noise ratio, with NEMD it is necessary to use strain rates g which are high enough to cause the shear viscosity to be strain rate dependent. In order to compute the shear viscosity of a Newtonian fluid using the sllod algorithm, after the simulation reaches the steady state at a given strain rate γ one computes and averages the pressure tensor defined in Eq. (8). The strain rate dependent shear viscosity is then obtained from Newton's law of viscosity

$$\eta = \frac{p_{xy} + p_{yx}}{2\gamma} \tag{9}$$

where p_{xy} and p_{yx} are the averaged xy and yx components of **P**. From kinetic and mode coupling theories, it is known [13–15] that to leading order the strain rate dependence of the shear viscosity is linear in $\gamma^{1/2}$. Hence, to apply the sllod algorithm to a Newtonian fluid, one performs several simulations at differing strain rates g and fits the resulting strain dependent viscosities to the equation

$$\eta = \eta(0) + \eta_1 \gamma^{1/2} \tag{10}$$

The zero strain rate extrapolation of η, $\eta(0)$, is thus the Newtonian viscosity.

III. RESULTS

The results are summarized in Table II for the pure dumbbell Ar system at $T = 135\,\mathrm{K}$ and $\rho = 1.034\,\mathrm{g/cm^3}$ and in Table III for the pure dumbbell Kr

TABLE II The pressure(p in bar), LJ energy(E_{LJ} in kJ/mole), and viscosity(η in $10^{-7}\,N\cdot s/m^2$) of the pure dumbbell Ar system as functions of strain rate(γ in ps^{-1}) and interatomic separation at $T=135\,K$ and $\rho=1.034\,g/cm^3$. These units are used for the pressure, energy, and viscosity in all the remaining tables

		$L=0$			$L=1/5$			$L=1/3$			$L=1/2$		
γ	*Run length*	p	$-E_{LJ}$	η	p	$-E_{LJ}$	η	p	$-E_{LJ}$	η	p	$-E_{LJ}$	η
1.0	60 k	188.5	4.034	661.2	234.9	2.897	501.5	397.7	2.325	481.7	565.6	1.879	462.9
0.81	60 k	135.7	4.093	675.9	186.0	2.937	515.7	351.7	2.349	492.2	522.3	1.891	476.2
0.64	60 k	64.9	4.142	695.9	164.8	2.959	525.1	327.4	2.373	502.8	492.3	1.910	481.2
0.49	100 k	47.1	4.161	712.2	126.8	2.983	540.2	301.9	2.401	516.3	476.7	1.933	491.2
0.36	100 k	31.0	4.174	725.1	127.8	2.997	555.8	295.0	2.418	526.1	460.1	1.940	504.8
0.25	100 k	27.3	4.183	746.6	123.3	3.007	564.2	287.5	2.421	537.0	451.2	1.952	518.2
0.16	160 k	18.0	4.198	764.8	119.1	3.012	574.5	269.0	2.429	554.8	434.9	1.957	530.3
0.09	160 k	16.9	4.206	783.3	124.7	3.016	585.7	261.8	2.440	565.6	433.0	1.960	546.9
0.04	200 k	12.0	4.207	791.8	113.4	3.018	597.2	242.8	2.459	578.1	438.5	1.967	553.1

TABLE III The pressure, LJ energy, and viscosity of the pure dumbbell Kr system as functions of strain rate and interatomic separation at $T = 135\,\mathrm{K}$ and $\rho = 2.315\,\mathrm{g/cm^3}$. Units and symbols are defined in Table II

		$L=0$			$L=1/5$			$L=1/3$			$L=1/2$		
γ	*Run length*	p	$-E_{LJ}$	η	p	$-E_{LJ}$	η	p	$-E_{LJ}$	η	p	$-E_{LJ}$	η
1.0	60 k	987.4	7.247	1571	614.6	5.275	1266	921.4	4.219	1176	1319	3.343	1167
0.81	60 k	843.7	7.351	1765	429.0	5.381	1314	732.2	4.341	1211	1095	3.472	1199
0.64	60 k	450.2	7.615	1984	284.6	5.489	1373	593.4	4.429	1262	976.2	3.551	1240
0.49	100 k	285.6	7.732	2126	174.9	5.563	1417	474.9	4.505	1301	832.0	3.633	1279
0.36	100 k	144.4	7.826	2295	62.3	5.629	1476	391.1	4.551	1341	760.2	3.681	1319
0.25	100 k	111.5	7.849	2440	29.0	5.660	1511	323.6	4.599	1379	693.2	3.725	1343
0.16	160 k	44.7	7.882	2648	12.2	5.691	1546	313.7	4.609	1408	674.3	3.737	1380
0.09	160 k	21.3	7.907	2849	−4.8	5.689	1583	290.2	4.626	1434	652.3	3.749	1398
0.04	200 k	19.3	7.905	2962	−19.2	5.702	1614	287.1	4.632	1466	650.9	3.751	1421

system at the same simulation state point. The pressure, LJ energy, and shear viscosity are reported as a function of strain rate (γ). The shear viscosity is shown as a function of $\gamma^{1/2}$ for the pure dumbbell Ar in Figure 1 and for the pure dumbbell Kr in Figure 2. The trend of the computed viscosities as a function of $\gamma^{1/2}$ for both pure dumbbell systems is almost the same as that for both pure spherical systems [1]: the computed viscosities fit the theoretical relationship, Eq. (10), quite well, and the slopes of viscosities against $\gamma^{1/2}$ for the pure dumbbell Kr systems are much steeper than those for the pure dumbbell Ar systems. The second feature is mainly due to the slopes of viscosities for the spherical Ar and Kr as shown in the cases of $L=0$ in Figures 1 and 2.

The zero strain rate extrapolations of the shear viscosity, shown as least-squares fitted straight lines in Figures 1 and 2, are used to determine the values of the shear viscosity which are reported in Table IV for the pure dumbbell Ar and Table V for the pure dumbbell Kr. Also presented in Tables IV and V are the density and energy as a function of interatomic separation at $T=135\,\mathrm{K}$ and $\rho=1.034\,\mathrm{g/cm^3}$. The ratio ($\eta/\eta_o$) of the shear viscosity of the pure dumbbell systems (η) to that of the spherical system (η_o) is also listed in Tables IV and V. As L increases from zero (spherical Ar) to 1/5, 1/3, and 1/2 (dumbbell Ar), the LJ energy decreases, indicating

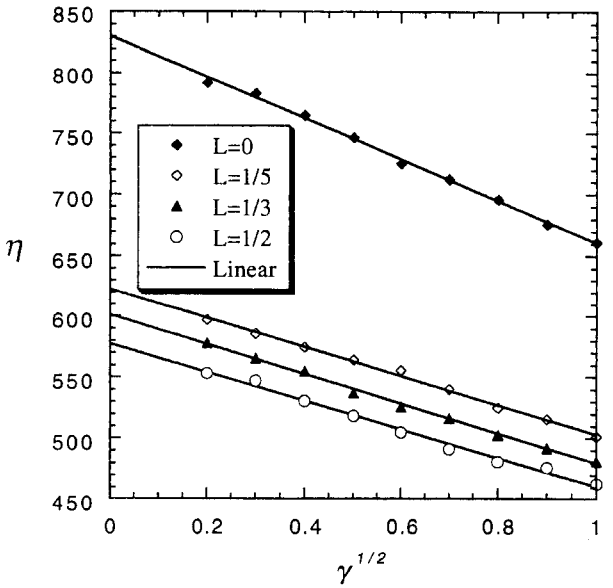

FIGURE 1 Shear viscosities (η in units of $10^{-7}\,\mathrm{N\cdot s/m^2}$) for pure dumbbell Ar system as a function of the square root of the strain rate (γ in units of $\mathrm{ps}^{-1/2}$) at $T=135\,\mathrm{K}$ and $\rho=1.034\,\mathrm{g/cm^3}$. The straight lines are least squared linear fits to the simulation results.

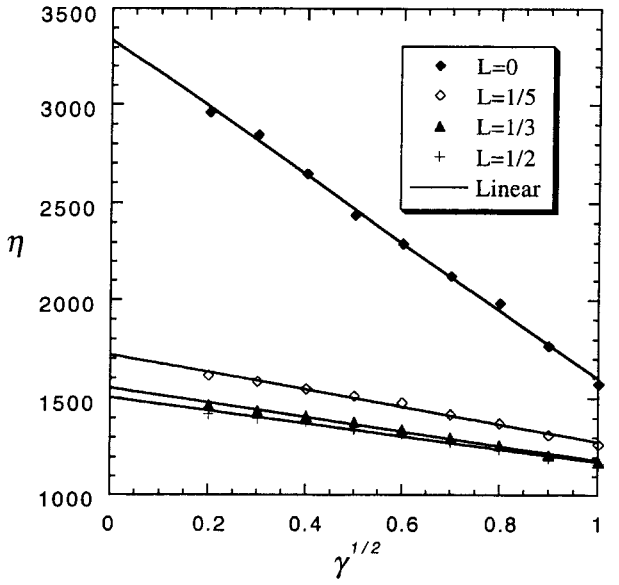

FIGURE 2 Shear viscosities (η in units of 10^{-7}N·s/m^2) for pure dumbbell Kr system as a function of the square root of the strain rate (γ in units of ps$^{-1/2}$) at $T=135$ K and $\rho=2.315$ g/cm^3. The straight lines are least squared linear fits to the simulation results.

TABLE IV The pressure, LJ energy, and viscosity of the pure dumbbell Ar system as a function of iteratomic separation at $T=135$ K and $\rho=1.034$ g/cm^3. Units and symbols are defined in Table II (η is obtained from least-squares linear fits to the simulation results)

Properties	L	p	$-E_{LJ}$	η	η/η_o
NVT MD	0	5.6	4.212	830.2	1.0000
NVT MD	1/5	110.5	3.021	622.7	0.7501
NVT MD	1/3	273.6	2.436	601.3	0.7243
NVT MD	1/2	426.6	1.977	577.0	0.6950

TABLE V The pressure, LJ energy, and viscosity of the pure dumbbell Kr system as a function of interatomic separation at $T=135$ K and $\rho=2.315$ g/cm^3. Units and symbols are defined in Table II (η is obtained from least-squares linear fits to the simulation results)

Properties	L	p	$-E_{LJ}$	η	η/η_o
NVT MD	0	20.1	7.898	3339	1.0000
NVT MD	1/5	30.4	5.697	1720	0.5151
NVT MD	1/3	290.3	4.632	1552	0.4648
NVT MD	1/2	626.0	3.763	1501	0.4495

dumbbell molecules repel each other, and this causes the pressure to decrease and consequently the shear viscosity to decrease. This result is expected from the experimental observation that the viscosity of normal

butane is less than that of isobutane. In Figure 3, The ratio (η/η_o) of the shear viscosity of the pure dumbbell systems (η) to that of the spherical system (η_o) is shown as a function of interatomic separation, L. It is apparent that the shear viscosity ratio for both pure dumbbell systems is essentially linearly decreased with increasing L except $L=0$, with a slightly large slope in the case of dumbbell Kr.

The strain rate dependent pressures, LJ energies, and viscosities of two mixtures – spherical Ar/dumbbell Kr system ($L_{Kr}=1/2$, referred to as case B) and dumbbell Ar/dumbbell Kr ($L_{Ar}=1/5$ and $Q_{Kr}=1/2$, referred to as case C) – are given in Tables VI and VII increasing in steps of 1/6 in the dumbbell Kr mole fraction x. The densities for both mixtures are determined by $\rho=[(1-x)\rho_{A\rho}+x\rho_{K\rho}]$. The viscosities of both mixture systems are plotted as a function of square root of strain rate, $\gamma^{1/2}$, in Figures 4 and 5. As in the case of spherical mixture system [1], the computed viscosities for both dumbbell systems fit the theoretical relationship, Eq. (10), quite well. The zero strain rate extrapolations of the shear viscosity, shown as least-squares fitted straight lines in Figures 4 and 5, are used to determine the values of the shear viscosity reported in Table VIII for the spherical/dumbbell mixture and Table IX for the dumbbell/dumbbell mixture along with pressures and LJ energies as a function of mole fraction of dumbbell Kr.

The composition dependent shear viscosities, LJ energies, and pressures for the two mixtures (cases B and C) are shown in Figures 6–8. For ideal liquid mixtures, the linear dependence of the properties on composition

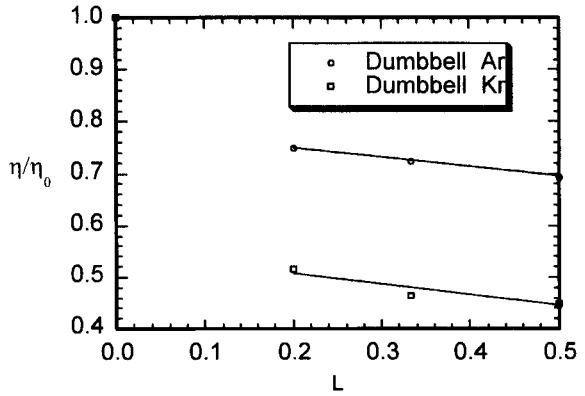

FIGURE 3 Shear viscosities (in units of 10^{-7} N·s/m^2) for the pure dumbbell Ar as a function of interatomic separation at $T=135$ K and $\rho=1.034$ g/cm^3. The linear curve is fitted to the simulation results.

TABLE VI The pressure, LJ energy, and viscosity of spherical Ar/dumbbell Kr ($L = 1/2$) mixture as functions of strain rate and dumbbell Kr mole fraction x at $T = 135$ K and $\rho = (1.034(1-x)+2.315x)$ g/cm^3. Units and symbols are defined in Table II

		$x=1/6$			$x=1/3$			$x=1/2$			$x=2/3$			$x=5/6$		
γ	*Run length*	p	$-E_{LJ}$	η	p	$-E_{LJ}$	η	p	$-E_{LJ}$	η	p	$-E_{LJ}$	η	p	$-E_{LJ}$	η
1.0	60 k	1089	3.510	724.6	864.2	3.662	776.3	666.0	3.792	845.1	499.0	3.915	984.9	328.6	3.989	1058
0.81	60 k	913.4	3.617	754.5	730.4	3.755	821.6	547.7	3.874	908.5	375.0	3.987	1031	270.5	4.038	1099
0.64	60 k	765.1	3.703	785.8	597.5	3.831	856.7	465.9	3.938	946.2	306.3	4.037	1060	192.4	4.101	1140
0.49	100 k	685.8	3.760	816.8	517.0	3.892	880.1	397.4	3.985	973.0	260.4	4.081	1093	153.4	4.141	1181
0.36	100 k	623.3	3.796	838.7	446.1	3.910	918.7	347.7	4.023	995.5	243.0	4.103	1132	124.7	4.165	1219
0.25	100 k	579.5	3.828	869.8	416.7	3.953	947.4	335.9	4.037	1021	188.2	4.126	1168	98.7	4.175	1251
0.16	160 k	535.8	3.856	907.5	411.4	3.966	976.5	296.8	4.051	1074	182.0	4.135	1207	86.8	4.189	1274
0.09	160 k	523.6	3.864	947.0	403.0	3.971	1009	275.4	4.057	1104	166.4	4.141	1226	54.1	4.215	1298
0.04	200 k	510.2	3.873	974.6	380.2	3.982	1050	270.9	4.060	1139	164.3	4.148	1265	74.9	4.205	1330

TABLE VII The pressure, LJ energy, and viscosity of dumbbell Ar ($L=1/5$)/dumbbell Kr ($L=1/2$) mixture as functions of strain rate and dumbbell Kr mole fraction x at $T=135\,\mathrm{K}$ and $\rho=(1.034(1-x)+2.315\,x)\,\mathrm{g/cm^3}$. Units and symbols are defined in Table II

		$x=1/6$			$x=1/3$			$x=1/2$			$x=2/3$			$x=5/6$		
γ	*Run length*	p	$-E_{LJ}$	η	p	$-E_{LJ}$	η	p	$-E_{LJ}$	η	p	$-E_{LJ}$	η	p	$-E_{LJ}$	η
1.0	60 k	1049	3.308	588.2	819.7	3.259	670.4	609.3	3.204	764.5	459.0	3.122	865.9	333.0	3.008	1031
0.81	60 k	887.9	3.409	605.2	692.9	3.342	701.0	522.3	3.257	794.1	370.1	3.180	896.6	273.8	3.055	1071
0.64	60 k	766.7	3.481	613.6	602.5	3.406	710.7	430.7	3.321	824.0	323.0	3.212	928.9	230.5	3.097	1104
0.49	100 k	663.9	3.546	646.9	529.5	3.451	737.1	384.8	3.360	846.3	287.3	3.240	951.8	213.9	3.118	1133
0.36	100 k	609.5	3.586	663.8	466.0	3.489	752.4	363.9	3.385	864.7	262.5	3.266	982.6	192.5	3.127	1170
0.25	100 k	544.0	3.625	688.8	438.2	3.511	778.5	334.6	3.401	884.4	253.2	3.282	999.5	184.4	3.144	1204
0.16	160 k	534.7	3.635	708.5	421.9	3.529	802.2	310.3	3.416	901.0	236.0	3.290	1041	172.4	3.154	1232
0.09	160 k	516.5	3.643	737.7	418.7	3.535	827.1	304.5	3.423	927.9	230.6	3.298	1070	165.1	3.158	1254
0.04	200 k	515.2	3.647	766.0	394.9	3.538	854.0	315.1	3.419	956.4	228.4	3.294	1096	154.8	3.164	1283

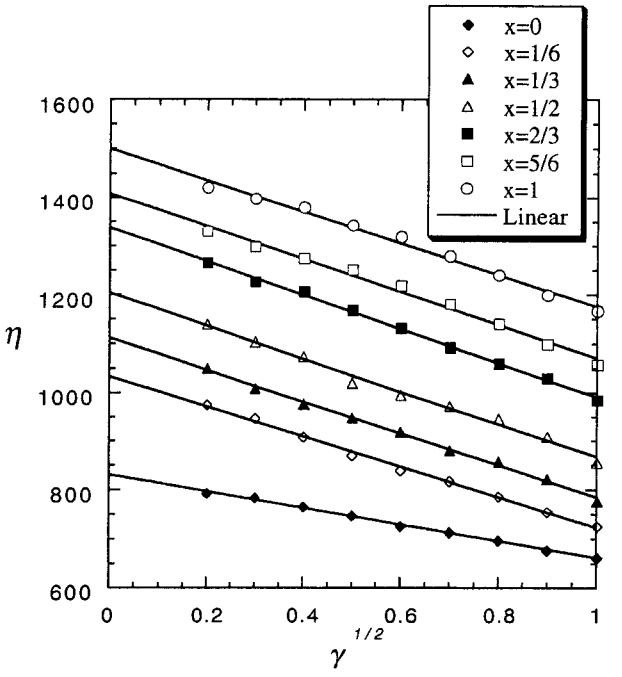

FIGURE 4 Strain rate dependence of the shear viscosities (η in units of 10^{-7} N·s/m^2) for spherical Ar/dumbbell Kr ($L=1/2$) mixture as a function of the square root of the strain rate (γ in units of ps$^{-1/2}$) at $T=135$ K and $\rho=(1.034(1-x)+2.315x)$ g/cm^3. The straight lines are least squared linear fits to the simulation results.

would be expected, *i.e.*,

$$P = x_1 P_1 + (1 - x_1) P_2 \tag{11}$$

where P is η, E, and p. From Figure 6 it is clear that for both spherical/dumbbell (case B) and dumbbell/dumbbell (case C), the viscosities are described quite well by the ideal liquid mixture expression. The ideality in case C is much better than in case B which is consistent with the idea that dumbbell/dumbbell mixtures are likely to be more ideal than spherical/dumbbell mixtures.

The LJ energies for each case are shown in Figure 7 as a function of the dumbbell Kr mole fraction x. The LJ energies for both case B and case C are described quite well by the ideal liquid mixture expression. The ideality in case C is also much better than in case B due to the same idea. As x increases from 0 (pure spherical Ar) to 1 (pure dumbbell Kr) in case B, the LJ energy decreases, but the pressure and the viscosity increase while as x increases

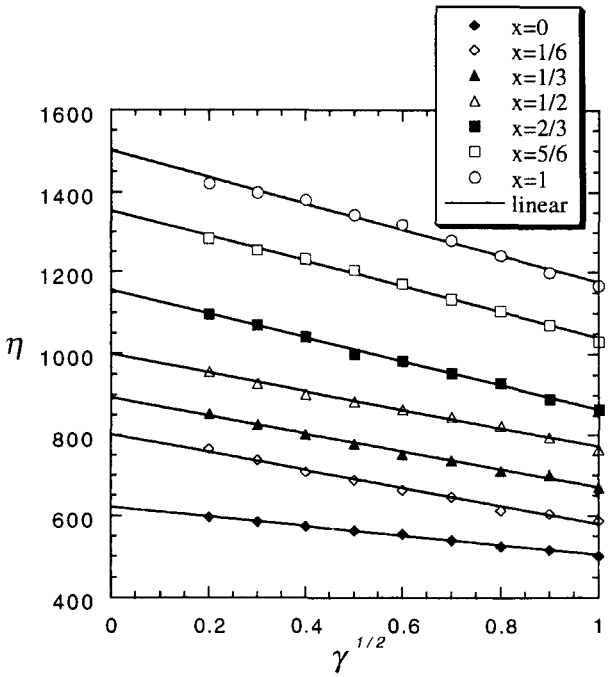

FIGURE 5 Strain rate dependence of the shear viscosities (η in units of 10^{-7} N·s/m^2) for dumbbell Ar ($L=1/5$)/dumbbell Kr ($L=1/2$) mixture as a function of the square root of the strain rate (γ in units of ps$^{-1/2}$) at $T=135$ K and $\rho=(1.034(1-x)+2.315x)$ g/cm^3. The straight lines are least squared linear fits to the simulation results.

TABLE VIII The pressure, LJ energy, and viscosity of spherical Ar/dumbbell Kr ($L=1/2$) mixture as a function of dumbbell Kr mole fraction x at $T=135$ K and $\rho=(1.034(1-x)+2.315x)$ g/cm^3. Units and symbols are defined in Table II

x	p	$-E_{LJ}$	η
1	626.0	3.763	1501
5/6	517.4	3.869	1408
2/3	388.5	3.978	1337
1/2	280.9	4.065	1207
1/3	185.1	4.137	1112
1/6	93.3	4.193	1034
0	5.6	4.212	830.2

from 0 (pure dumbbell Ar) to 1 (pure dumbbell Kr) in case C, the LJ energy, the pressure, and the viscosity increase.

The mixture pressures are shown in Figure 8 for both cases along with the ideal liquid mixture prediction. The spherical/dumbbell mixture (case B) is

TABLE IX The pressure, LJ energy, and viscosity of dumbbell Ar ($L=1/5$)/dumbell Kr ($L=1/2$) mixture as a function of dumbbell Kr mole fraction x at $T=135\,\mathrm{K}$ and $\rho=(1.034(1-x)+2.315x)\,\mathrm{g/cm^3}$. Units and symbols are defined in Table II

x	p	$-E_{LJ}$	η
1	626.0	3.763	1501
5/6	527.4	3.643	1353
2/3	386.3	3.541	1153
1/2	309.6	3.416	998.7
1/3	236.9	3.300	893.0
1/6	167.0	3.168	802.8
0	110.5	3.021	622.7

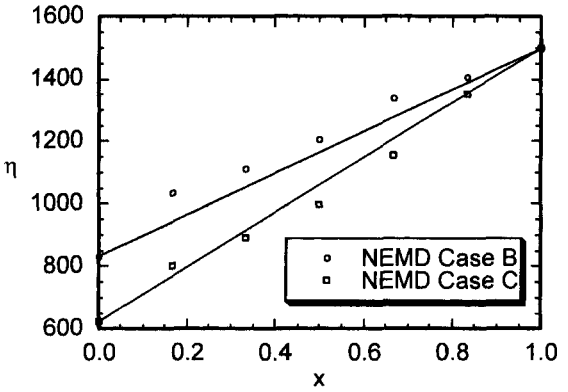

FIGURE 6 Composition dependence of the shear viscosity of Ar/Kr mixtures (B: spherical/dumbbell, C: dumbbell/dumbbell). In each case, the straight line is the linear dependence expected in the case of ideal liquid mixtures.

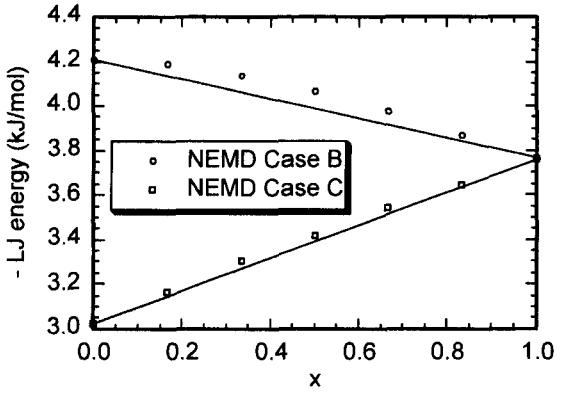

FIGURE 7 Composition dependence of the LJ energy of Ar/Kr mixtures (B: spherical/dumbbell, C: dumbbell/dumbbell). In each case, the straight line is the linear dependence expected in the case of ideal liquid mixtures.

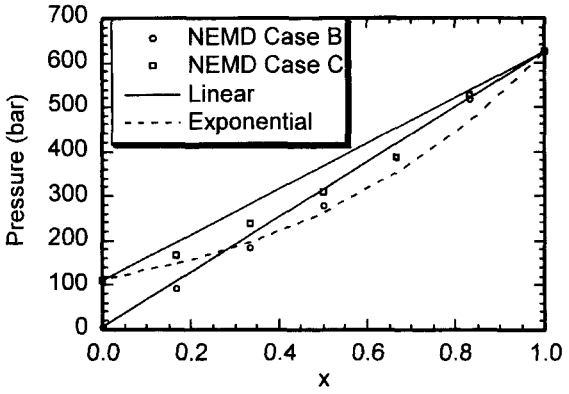

FIGURE 8 Composition dependence of the pressure of Ar/Kr mixtures (B: spherical/dumbbell, C: dumbbell/dumbbell). In each case, the straight line is the linear dependence expected in the case of ideal liquid mixtures. The dashed line is the exponential model described in the text.

described accurately by the ideal liquid mixture expression while the dumbbell/dumbbell mixture (case C) is not. This is not consistent with the better ideality of case C in the shear viscosity and the LJ energy than case B. A common engineering correlation for liquid mixture viscosities is given by [16]

$$\eta = \exp[x_1 \ln \eta_1 + (1 - x_1) \ln \eta_2] \tag{12}$$

The dashed curves in Figure 8 represent the prediction of Eq. (12). In the case of dumbbell/dumbbell mixtures, the pressures are described well by the logarithmic relationship.

IV. CONCLUSION

It is evident from all the results presented in this paper that the interaction between dumbbell molecules is less attractive than that between spherical molecules which leads to lower viscosities as was observed in the experimental fact that the viscosity of normal alkanes is less than that of branched alkanes. From the results of NEMD for two mixtures – spherical Ar/dumbbell Kr system (case B) and dumbbell Ar/dumbbell Kr (case C), the viscosities and the LJ energies of both mixture systems are described quite well by the liquid mixture expression. The ideality in case C is much better than in case B which is consistent with the idea that dumbbell/dumbbell mixtures are likely to be more ideal than spherical/dumbbell mixtures.

But the mixture pressures of the spherical/dumbbell mixture (case B) are described accurately by the ideal liquid mixture expression while those of the dumbbell/dumbbell mixture (case C) are not, which is not consistent with the better ideality of case C in the shear viscosity and the LJ energy than case B. In the case of dumbbell/dumbbell mixtures, the pressures are described well by the logarithmic dependence on the dumbbell Kr mole fraction x.

Acknowledgment

SHL thanks the Tongmyung University of Information Technology (Pusan, South Korea) for access to its IBM SP/2 computer. The work of PTC was supported by the Division of Chemical Sciences, Office of Basic Energy Sciences, U. S. Department of Energy.

References

[1] Lee, S. H. and Cummings, P. T. (1993). "Shear viscosity of model mixtures by nonequilibrium molecular dynamics. I. Argon–krypton mixtures", *J. Chem. Phys.*, **99**, 3919.
[2] Lee, S. H. and Cummings, P. T. (1994). "Shear viscosity of model mixtures by nonequilibrium molecular dynamics. II. Effect of dipolar interaction", *J. Chem. Phys.*, **101**, 6206.
[3] Lee, S. H. and Cummings, P. T. (1996). "Effect of three-body forces on the viscosity of liquid argon", *J. Chem. Phys.*, **105**, 2044.
[4] Lee, S. H. and Cummings, P. T. (2001). "Shear viscosity of model mixtures by nonequilibrium molecular dynamics. III. Effect of quadrupolar interaction".
[5] Barker, J. A., Fisher, R. A. and Watts, R. O. (1971). "Liquid argon: Monte Carlo and molecular dynamics calculations", *Mol. Phys.*, **21**, 657.
[6] Barker, J. A., Watts, R. O., Lee, J. K., Schafer, T. P. and Lee, Y. T. (1974). "Interatomic potentials for krypton and xenon", *J. Chem. Phys.*, **61**, 3081.
[7] Alien, M. P. and Tildesley, D. J., *Computer Simulation of Liquids* (Oxford University, Oxford, 1987), p. 334.
[8] Allen, M. P. and Tildesley, D. J., *Computer Simulation of Liquids* (Oxford University, Oxford, 1987), p. 332.
[9] Evans, D. J. (1977). "On the representation of orientation space", *Mol. Phys.*, **34**, 317.
[10] Evans, D. J. and Murad, S. (1977). "Singularity free algorithm for molecular dynamics simulation of rigid polyatomics", *Mol. Phys.*, **34**, 327.
[11] Lees, A. W. and Edwards, S. F. (1972). "The computer study of transport processes under extreme conditions", *J. Phys. C: Solid State*, **5**, 1921.
[12] Evans, D. J. and Morriss, G. P. (1984). "Nonlinear response theory for steady planar Couette flow", *Phys. Rev. A*, **30**, 1528.
[13] Yamada, T. and Kawasaki, K. (1975). "Application of mode coupling theory to nonlinear stress tensor in fluids", *Prog. Theor. Phys.*, **53**, 111.
[14] Kawasaki, K. and Gunton, J. D. (1973). "Theory of nonlinear transport processes: Nonlinear shear viscosity and normal stress effects", *Phys. Rev. A*, **8**, 2048.
[15] Ernst, M. H., Cichocki, B., Dorfman, J. R., Sharma, J. and van Beijeren, H. (1978). "Kinetic theory of nonlinear viscous flow in two and three dimensions", *J. Stat. Phys.*, **18**, 237.
[16] Reid, R. C., Prausnitz, J. M. and Sherwood, T. K., *The properties and Liquids and Gases* (McGraw-Hill, New York, 1977), 3rd edn.